Dynamic Nuclear Magnetic Resonance Study of the Effects of *cis*-Chelate Ligands on 1,2-Metallotropic Shifts in Trimethylplatinum(IV) Complexes of Pyridazine†

Edward W. Abel,[a] Peter J. Heard,[a] Keith G. Orrell,*[,a] Michael B. Hursthouse[b] and K. M. Abdul Malik[b]

[a] *Department of Chemistry, The University, Exeter EX4 4QD, UK*

[b] *Department of Chemistry, University of Wales, Cardiff, PO Box 912, Cardiff CF1 3TB, UK*

The complexes *fac*-$[PtMe_3(L\text{–}L)(pydz)][BF_4]$ (L–L = neutral bidentate chelate ligand; pydz = pyridazine) were readily prepared from *fac*-$[PtIMe_3(L\text{–}L)]$ by the action of silver(I) salts in the presence of an excess of pyridazine. Pyridazine is acting as a monodentate ligand, which undergoes a facile 1,2-metallotropic shift between the two equivalent, contiguous nitrogen donor atoms. The solution-state stereodynamics of these complexes have been elucidated by two-dimensional exchange spectroscopy and accurate activation parameters deduced. Energy barriers [$\Delta G^{\ddagger}$ (298 K)] are in the range 58–78 kJ mol^{-1}. The effects of the chelate ligand on the energetics of the fluxional shift are discussed and rationalised. The crystal structure of *fac*-$[PtMe_3(bipy)(pydz)][BF_4]$ (bipy = 2,2′-bipyridyl) was determined to confirm the *fac*-octahedral co-ordination geometry of the complexes.

Azines are highly versatile donors which form an extensive variety of co-ordination compounds.[1] When the azine possesses a contiguous pair of nitrogen donor atoms the possibility of a 1,2-metallotropic shift arises. Pyridazine (pydz) is illustrative of this case. The latent fluxionality of metal–pyridazine complexes has been investigated previously, in order to elucidate the potential stereodynamic behaviour of such systems.[2–8]

We have reported recently on the fluxionality associated with the bis(pyridazine) complexes of the halogenotrimethylplatinum(IV) compounds, *viz.* *fac*-$[PtXMe_3(pydz)_2]$ (X = Cl, Br or I).[6,8] The halogenotrimethylplatinum(IV) moiety can be readily dehalogenated with silver(I) salts in the presence of a donor ligand to form complexes of general formula *fac*-$[PtMe_3L_2L']^+$ (where L and L′ may be the same or different). This paper describes the results of our studies on the effect of the chelate ligand on the 1,2-fluxional shift of pyridazine in the complexes *fac*-$[PtMe_3(L\text{–}L)(pydz)][BF_4]$ (where L–L is a neutral bidentate chelate ligand).

Experimental

Materials.—Iodotrimethylplatinum(IV) was prepared by standard procedures[9,10] and $[PtIMe_3(bipy)]$ (bipy = 2,2′-bipyridyl) was synthesised by the method of Clegg *et al.*[11] The proligands were obtained from standard sources (Aldrich Chemical Company or Lancaster Syntheses Ltd.) and used as supplied.

Synthesis of the Complexes.—All manipulations were carried out under an atmosphere of dry, oxygen-free nitrogen using standard Schlenk techniques.[12] All solvents were dried[13] and degassed prior to use. The complexes $[PtIMe_3(L\text{–}L)]$ [L–L = 1,10-phenanthroline (phen), 2,2′-bipyrimidine (bipym) and *N,N,N′N′*-tetramethylethylenediamine (tmen)] were all prepared in a similar fashion to that of $[PtIMe_3(bipy)]$.[11] Details of the synthesis of $[PtIMe_3(tmen)]$ are given below as an example.

Iodotrimethyl(N,N,N′,N′-*tetramethylethylenediamine*)-*platinum*(IV). *N,N,N′,N′*-Tetramethylethylenediamine (0.30 g, 2.58 mmol) was added to a stirred benzene solution (30 cm^3) of iodotrimethylplatinum(IV) (0.66 g, 1.81 mmol based on the monomeric unit). The reaction mixture was stirred at room temperature for *ca.* 4.5 h. The benzene solution was concentrated to *ca.* 5 cm^3 and an excess of hexane added. The resultant white solid was isolated and dried *in vacuo*. No further purification was necessary. Yield 0.68 g (78%).

The complexes $[PtMe_3(L\text{–}L)(pydz)][BF_4]$ (L–L = bipy, phen, bipym or tmen) were prepared *via* the same route; the case of $[PtMe_3(bipy)(pydz)][BF_4]$ is described below as an illustrative example.

(2,2′-*Bipyridyl*)*trimethyl*(*pyridazine*)*platinum*(IV) *tetrafluoroborate*. The complex $[PtIMe_3(bipy)]$ (1.0 g, 1.91 mmol) and silver tetrafluoroborate (0.50 g, 2.56 mmol) were stirred in tetrahydrofuran (thf) (40 cm^3) for *ca.* 1 h. The resulting solution was filtered (to remove AgI) and then added to a stirred thf solution (5 cm^3) of pyridazine (0.22 g, 2.76 mmol). After *ca.* 1 h of stirring at ambient temperature the resulting white solid was filtered off and dried *in vacuo*. Recrystallisation from ethyl methyl ketone–diethyl ether afforded 1.05 g (97%) of pure, crystalline $[PtMe_3(bipy)(pydz)][BF_4]$.

Physical Methods.—Hydrogen-1 NMR spectra were recorded as $(CD_3)_2C{=}O$ or D_2O–$(CD_3)_2C{=}O$ (1 : 1) solutions on a Bruker AM250 Fourier-transform spectrometer, operating at 250.13 MHz. Chemical shifts are quoted in ppm relative to tetramethylsilane as an internal standard. The NMR probe temperatures were controlled by a standard B-VT 1000 unit, and periodically checked against a digital thermometer (Comark); probe temperatures are considered accurate to ± 1 °C. Two-dimensional exchange (EXSY) spectra were measured using the Bruker automation program NOESYPH,[14] which generates the pulse sequence D_1–90°–D_0–90°–D_9–90°–free induction decay. The relaxation delay, D_1, was 2.0 s, and the evolution time, D_0, had an initial value of 3 μs. Spectra were typically recorded with 512 words of data in each frequency domain, and transformed with 1024 words. Peak intensities were measured by volume integration of the resulting two-

† *Supplementary data available:* see Instructions for Authors, *J. Chem. Soc., Dalton Trans.*, 1995, Issue 1, pp. xxv–xxx.

Table 1 Synthetic and analytical data for the complexes $[PtMe_3(L\text{–}L)(pydz)][BF_4]$ (L–L = bipy, bipym, phen or tmen)

Complex (chelate ligand)	Yield[a] (%)	ν(C–H)[b]/cm^{-1}	ν(Pt–C)[b,c]/cm^{-1}	ν(Pt–N)[b]/cm^{-1}	Analysis[d] (%)	*m/z*[e]
bipy	97	2820.7s	575.3w	375.1w	C 36.35 (36.25)	476
		2900.3s	582.5w	419.7w	H 3.60 (3.75)	
		2966.1s			N 10.00 (9.95)	
bipym	13	2817.2s	576.9w	374.6w	C 30.30 (31.85)	478
		2898.9s		419.7w	H 3.30 (3.40)	
		2965.6s			N 13.40 (14.85)	
phen	19	2819.3s		374.8w	C 38.50 (38.85)	500
		2900.3s		376.3 (sh)	H 3.15 (3.60)	
		2965.3s			N 9.65 (9.55)	
tmen	71	2817.8s	560.8w	373.4w	C 29.85 (29.85)	435[f]
		2899.9s	569.8w	396.2w	H 5.65 (5.60)	
		2979.0s			N 10.75 (10.70)	

[a] Relative to $[PtXMe_3(L\text{–}L)]$. [b] Infrared spectra recorded as CsI discs; s = strong, w = weak, sh = shoulder. [c] Not all bands observed. [d] Calculated values in parentheses. [e] Mass spectrometry data. Parent ion due to $[M - BF_4]^+$, except for the tmen complex. [f] Ion observed due to $[M - H - BF_4]^+$.

dimensional spectrum. Integrations were performed at least five times on each of the spectra and the mean value was used to calculate the exchange rate using the D2DNMR program, as detailed previously.[15] Five EXSY experiments were carried out at different temperatures on each of the complexes and the subsequent data were used to determine the activation parameters from a least-squares fit of the Eyring and Arrhenius plots. The errors quoted are those defined by Binsch and Kessler.[16]

Infrared spectra were recorded as pressed CsI discs on a Nicolet Magna 550 FT-IR spectrometer, equipped with a CsI beam splitter, operating in the region 4000–200 cm^{-1}. Fast atom bombardment (FAB) mass spectra were obtained by Dr J. A. Ballantine (courtesy of the Swansea EPSRC service) on a VG AutoSpec instrument using caesium-ion bombardment at 25 kV energy on the complexes dissolved in a matrix of 3-nitrobenzyl alcohol. Elemental analyses were carried out by Butterworth Laboratories Ltd., Teddington, Middlesex.

Crystal Structure Determination of $[PtMe_3(bipy)(pydz)][BF_4]$.—*Crystal data.* $C_{17}H_{21}BF_4N_4Pt$, $M_r = 563.29$, monoclinic, space group $C2/c$, $a = 23.901(4)$, $b = 10.659(2)$, $c = 16.502(5)$ Å, $\beta = 106.423(8)°$, $U = 4033(2)$ Å^3 (by least-squares refinement of 250 reflections within $1.78 \leqslant \theta \leqslant 24.90°$), $Z = 8$, $D_c = 1.856$ g cm^{-3}, $F(000) = 2160$, Mo-Kα radiation, $\lambda = 0.710\,69$ Å, $\mu = 70.0$ cm^{-1}, $T = 293$ K, colourless tablets, crystal size 0.35 × 0.15 × 0.10 mm.

Data collection and processing. Intensity data were collected using a FAST TV area detector diffractometer situated at the window of a rotating-anode generator (molybdenum anode), as described previously.[17] The total number of reflections recorded was 6134 [$1.78 \leqslant \theta \leqslant 24.90°$; $-8 \leqslant h \leqslant 26$, $-11 \leqslant k \leqslant 8$, $-17 \leqslant l \leqslant 14$], giving 3020 unique ($R_{int} = 0.0726$ after absorption correction, maximum and minimum absorption correction factors = 1.117 and 0.913).

Structure analysis and refinement. The structure was solved by Patterson methods and refined by full-matrix least squares on F_o^2 using all 3020 unique data. All non-hydrogen atoms were anisotropic. The hydrogen atoms were allowed to ride on their parents with $U_{iso} = nU_{eq}$ of the parent ($n = 1.2$ for CH and 1.5 for CH_3). The weighting scheme used was $w = 1/\sigma^2(F_o^2)$. Three fluorine atoms of the BF_4 anion were disordered and refined with partial occupancies. The B–F distances were constrained to refine to the same value. Final wR_2 (on F_o^2) and R (on F) values were 0.1206 and 0.0595 for 275 parameters and all 3020 data. The corresponding values for 1774 data with $I > 2\sigma(I)$ were 0.0994 and 0.0406 respectively. All calculations were performed on a 486 DX2/66 personal computer using programs given in ref. 18. Sources of scattering factors were as in SHELXL 93.

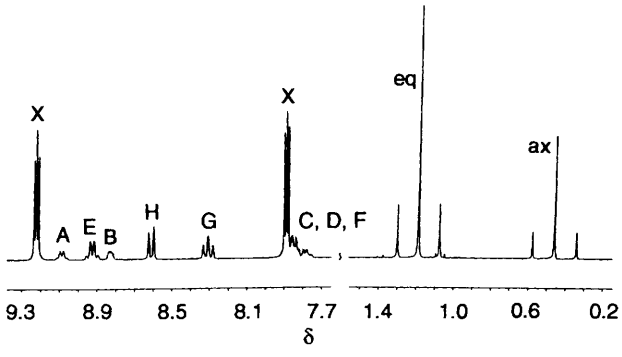

Fig. 1 The 250 MHz ^{1}H NMR spectrum of $[PtMe_3(bipy)(pydz)][BF_4]$ in D_2O–$(CD_3)_2CO$ (1:1 v/v) at 303 K. For labelling see Scheme 1. Signals denoted by X are due to free pyridazine

Fractional atom coordinates and selected bond lengths and angles are given in Tables 6 and 5 respectively.

Additional material available from the Cambridge Crystallographic Data Centre comprises H-atom coordinates, thermal parameters, and remaining bond lengths and angles.

Results

The complexes $[PtMe_3(L\text{–}L)(pydz)][BF_4]$ (L–L = bipy, phen, bipym or tmen) were isolated as white or cream-white, air-stable (except L–L = bipym) crystalline solids as described (see above). Their infrared spectra each comprised three main bands in the C–H stretching region; two due to C–H stretching modes and one to the overtone of the C–H deformation mode at *ca.* 1410 cm^{-1}. Bands due to the two Pt–C and two Pt–N stretching modes could be tentatively assigned in most cases (Table 1). The infrared data are consistent with the $PtMe_3$ moiety having a *fac*-octahedral co-ordination geometry.[11,19–21] Fast atom bombardment mass spectrometry was performed on the complexes; in most cases (L–L = bipy, phen or bipym) molecular ions were observed for the species $[M - BF_4]^+$. In the case of $[PtMe_3(tmen)(pydz)][BF_4]$ the molecular ion corresponded to $[M - H - BF_4]^+$. In all cases, the observed isotope patterns were consistent with those calculated for the formulated species. With the exception of $[PtMe_3(bipym)(pydz)][BF_4]$, elemental analyses indicated the formation of analytically pure samples. The somewhat low C, H and N analyses obtained for the latter are presumed to result from partial decomposition of the complex (see above). Analytical data for the four complexes $[PtMe_3(L\text{–}L)(pydz)][BF_4]$ (L–L = bipy, phen, bipym or tmen) are reported in Table 1.

Table 2 Hydrogen-1 NMR data[a] for the complexes $[PtMe_3(L\text{–}L)(pydz)][BF_4]$ (L–L = bipy, bipym, phen or tmen)

Complex (chelate ligand)	Solvent	T/K	δ(Pt–CH_3)[b]	δ(pydz H)[c]	δ(chelate H)[c]
bipy	D_2O–$(CD_3)_2CO$ (1 : 1 v/v)	303	0.56 (71.0) (ax) 1.19 (67.5) (eq)	A 9.09 (5.2) B 8.82 C 7.8 D 7.8	E 8.93 (6.3) (18.1)[d] F 7.8 G 8.31 (7.9, 8.2) H 8.61 (8.2)
bipym	$(CD_3)_2CO$	303	0.72 (70.3) (ax) 1.40 (69.3) (eq)	A 9.28 B 8.91 C 8.0 D 7.9	E 9.4 F 8.15 G 9.4
phen	$(CD_3)_2CO$	303	0.55 (70.7) (ax) 1.44 (68.1) (eq)	A 9.31 (5.3) (16)[d] B 8.84 (4.3) C 7.9 D 7.8	E 9.45 (5.1) (13.3)[d] F 8.31 (8.3, 5.1) G 9.01 (8.3) H 8.34
tmen	$(CD_3)_2CO$	253	0.91 (69.6) (ax) 0.97 (65.8) (eq)	A 9.29 (4.9) (14)[d] B 9.56 C 8.2 D 8.2	Me(*cis*) 2.55 (17.7)[d] Me(*trans*) 2.60 (9.4)[d] H(*cis*) 3.0[e] H(*trans*) 3.5[e]

[a] Chemical shifts quoted relative to $SiMe_4$ as an internal standard. [b] ^2J(PtH)/Hz in parentheses; ax = axial, eq = equatorial. [c] Labelling refers to Schemes 1 and 3; ^3J(HH)/Hz in parentheses; not all scalar couplings resolved. [d] ^3J(PtH)/Hz. [e] Assignment uncertain (see text).

NMR Studies.—(*i*) *Complexes* $[PtMe_3(L\text{–}L)(pydz)][BF_4]$ (L–L = *bipy, phen or bipym*). The ambient-temperature (303 K) solution ^1H NMR spectra of the complexes $[PtMe_3(L\text{–}L)(pydz)][BF_4]$ (L–L = bipy, phen or bipym) exhibited well resolved signals, consistent with pyridazine acting as a non-exchanging, monodentate ligand (see below). The spectra comprised two regions: (*i*) the platinum–methyl region (*ca.* δ 0.5–1.5); (*ii*) the aromatic (ligand) region (*ca.* δ 7.8–9.5) (Table 2). The spectrum of $[PtMe_3(bipy)(pydz)][BF_4]$ is shown in Fig. 1.

The platinum–methyl regions of the spectra each comprised two sets of signals, with satellites due to ^{195}Pt–H scalar coupling, in a 1 : 2 intensity ratio. The relative intensities of the signals allowed them to be assigned unambiguously to the axial (*trans* pydz) and equatorial (*trans* chelate ligand) platinum–methyl environments, respectively. The ^3J(PtH) scalar coupling constants observed for the axial platinum–methyl groups were higher than those for their equatorial counterparts, indicating[22,23] that the chelate ligands exert a stronger *trans* influence than does pyridazine.

The aromatic regions of the ^1H NMR spectra each comprised two sets of signals, one set due to the four non-equivalent pyridazine hydrogen environments, and one due to the chelate ligand hydrogen atoms. The two sets of signals were distinguished unambiguously either by performing a series of selective homonuclear decoupling experiments or by homonuclear correlation spectroscopy (COSY). The highest-frequency signals in both sub-spectra displayed measurable ^{195}Pt scalar coupling, which enabled them to be assigned to the hydrogen atoms adjacent to the co-ordinated nitrogens (Scheme 1). The sub-spectra due to the pyridazine ring hydrogen atoms comprised three signals in a 1 : 1 : 2 intensity ratio, characteristic of pyridazine acting as a non-exchanging monodentate ligand.[6] The 3- and 6-position hydrogen environments, H_A and H_B, were distinguished by virtue of the measurable $^3J(PtH_A)$ scalar coupling (see above). The 4- and 5-position hydrogen atoms, H_C and H_D, have virtually identical chemical shifts and could not be distinguished unambiguously. The chelate ligand sub-spectra were assigned on the basis of their scalar coupling networks and by comparison with the ^1H NMR spectra of the free L–L.

On warming solutions of the complexes $[PtMe_3(L\text{–}L)(pydz)][BF_4]$ (L–L = bipy, phen or bipym) the signals due to H_A and H_B of the pyridazine ring exhibited reversible dynamic exchange broadening, indicating the onset of a 1,2-platinum–nitrogen shift process at a measurable rate. The close proximity of the bands due to H_C and H_D (Table 2) renders these signals insensitive to the chemical exchange process. The low boiling point of the solvents $[(CD_3)_2C{=}O$ or $(CD_3)_2C{=}O$–D_2O (1 : 1)] prevented the acquisition of a full set of variable-temperature spectra and so kinetic data were sought by two-dimensional exchange spectroscopy. Accordingly, five such experiments were run at different temperatures on each of the complexes and accurate rate data were extracted (Table 3). The two-dimensional EXSY spectrum of $[PtMe_3(bipym)(pydz)][BF_4]$ at 303 K is shown in Fig. 2. This clearly reveals the presence of cross-peaks between the signals due to H_A and H_B, resulting from the 1,2-Pt–N shift (Scheme 2). The activation parameters determined for the 1,2-fluxional shift process are reported in Table 4.

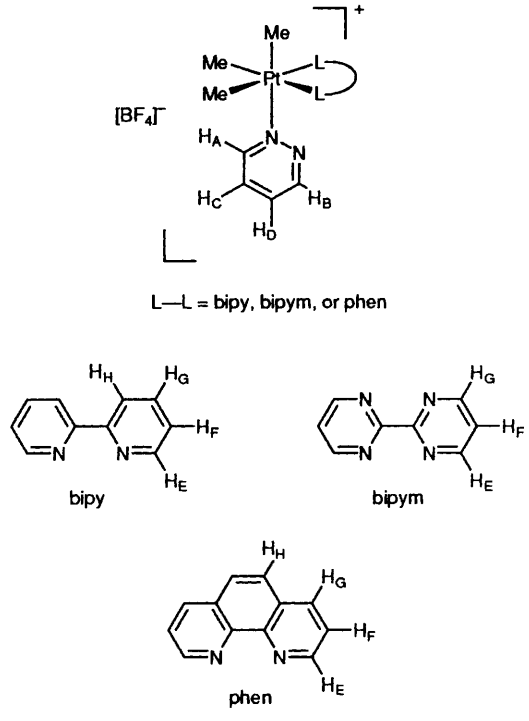

Scheme 1 The complexes $[PtMe_3(L\text{–}L)(pydz)][BF_4]$ (L–L = bipy, bipym or phen) showing the H-atom labelling in the ligands

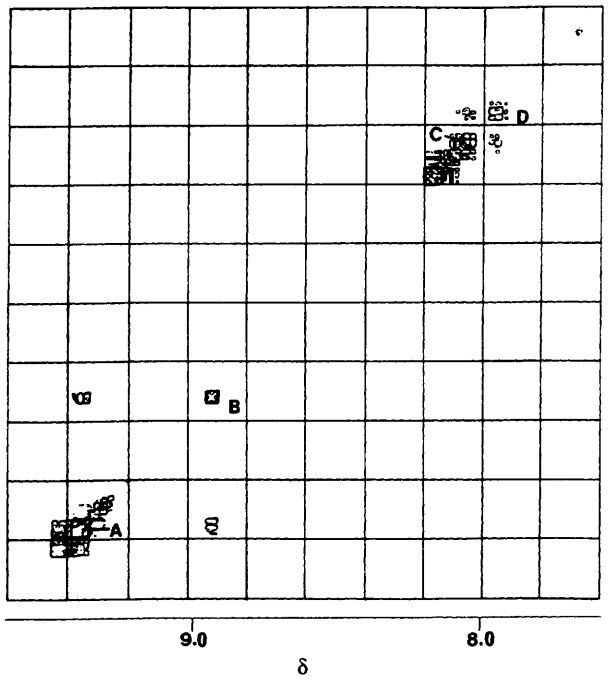

Fig. 2 The 250 MHz ^{1}H two-dimensional EXSY spectrum of $[PtMe_3(bipym)(pydz)][BF_4]$ at 303 K showing cross-peaks between the pyridazine hydrogens H_A, H_B and H_C, H_D

Table 3 Two-dimensional EXSY NMR data for the complexes $[PtMe_3(L\text{–}L)(pydz)][BF_4]$ (L–L = bipy, bipym, phen or tmen)

Complex (chelate ligand)	T/K	Rate */s^{-1}
bipy	293	0.35
	298	0.69
	303	0.87
	308	2.18
	313	3.20
bipym	298	0.13
	303	0.32
	308	0.87
	313	1.27
	323	5.41
phen	298	0.24
	303	0.43
	313	1.02
	318	2.44
	323	4.20
tmen	253	0.07
	258	0.27
	263	0.58
	268	1.71
	273	4.68

* First-order rate constants for the 1,2-metal–nitrogen shift process. Uncertainties *ca.* ± 10%.

(*ii*) *Complex* $[PtMe_3(tmen)(pydz)][BF_4]$. The ambient-temperature (303 K) ^{1}H NMR spectrum of this complex in $(CD_3)_2C{=}O$ solution exhibited broad, unresolved signals in the aromatic region (see below). On cooling to *ca.* 253 K these bands sharpened and a well resolved, static spectrum was obtained. The spectrum at 253 K (Fig. 3) consisted of three regions: (*i*) the platinum–methyl region (*ca.* δ 0.9–1.0); (*ii*) the *N*,*N*,*N*′,*N*′-tetramethylethylenediamine region (*ca.* δ 2.5–3.6); (*iii*) the aromatic (pydz) region (*ca.* δ 8.2–9.6).

The platinum–methyl region comprised three signals, with

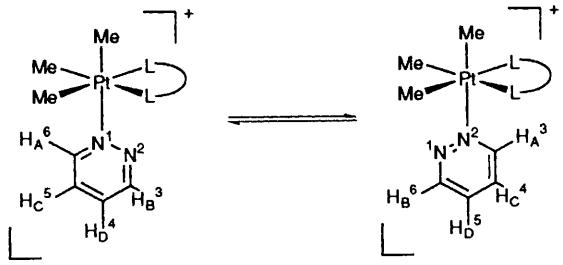

Scheme 2 Effects of the 1,2-metallotropic shift in $[PtMe_3(L\text{–}L)(pydz)][BF_4]$ complexes on the pydz hydrogens

platinum-195 satellites, in a 1:2 intensity ratio. These signals were assigned unambiguously to the axial (*trans* pydz) and equatorial (*trans* tmen) Pt–Me environments, respectively. The relative magnitudes of the scalar coupling constants $^2J(Pt\text{–}CH_{eq})$ and $^2J(Pt\text{–}CH_{ax})$ (Table 2) indicate that tmen exerts a stronger *trans* influence[22,23] than does pyridazine.

The aromatic region displayed three signals in 1:1:2 intensity ratio, assigned to H_B, H_A and $H_{C/D}$ of the pyridazine ring, respectively (Scheme 3); H_B and H_A were distinguished by virtue of the fact that H_A displayed measurable coupling to platinum-195. In contrast to the complexes $[PtMe_3(L\text{–}L)(pydz)][BF_4]$ (L–L = bipy, phen or bipym) (see above) and $[PtXMe_3(pydz)_2]$ (X = Cl, Br or I),[6] H_B was shifted to higher frequency than H_A, as a result of being deshielded. This substantial deshielding of H_B is difficult to rationalise.

The signals due to *N*,*N*,*N*′,*N*′-tetramethylethylenediamine comprised two equally intense singlets, with platinum-195 satellites, due to two inequivalent *N*-methyl groups, and two complex second-order multiplets due to the methylene hydrogen atoms. The lower frequency of the two *N*-methyl signals was attributed to the methyls *cis* to pyridazine (Scheme 3), since they would be expected to be slightly shielded relative to the *N*-methyls *trans* to pyridazine as a result of the influence of the aromatic ring current. The higher-frequency signal was thus assigned to the *trans* *N*-methyls. The $^2J(PtH)$ scalar coupling associated with the *cis* *N*-methyls was approximately double that associated with the *trans* *N*-methyls. This difference in the magnitudes of the scalar coupling interactions presumably arises because of differences in the dihedral angles between the Pt–N–C and N–C–H planes. The two methylene signals were not fully resolved and could not be assigned unambiguously.

On warming above 253 K, changes were observed in the aromatic (pyridazine) region of the spectra, indicative of a 1,2-metallotropic shift process leading to an exchange of H_A and H_B (Scheme 2). Protons H_C and H_D have almost identical chemical shifts (Table 2) and are therefore insensitive to the fluxional exchange. Standard one-dimensional band-shape analysis of the temperature-dependent spectra was frustrated by an intermolecular exchange with a minor solution-state species (denoted X in Fig. 3). Rate data were therefore obtained by two-dimensional EXSY experiments. The spectra were recorded at sufficiently low temperatures to prevent any magnetisation transfers due to the intermolecular exchange process, thus enabling rates of the specifically intramolecular 1,2-Pt–N shift to be measured. Five EXSY experiments were performed in the temperature range 253–273 K and reliable kinetic data for the 1,2-metallotropic shift were obtained (Table 3). The spectrum of $[PtMe_3(tmen)(pydz)][BF_4]$ at 258 K is shown in Fig. 4. The absence of any cross-peaks between the signal due to the minor species (denoted X) and the pyridazine signals clearly shows that the intermolecular exchange is of negligible rate at these temperatures. The activation parameters are reported in Table 4, along with those for the complexes $[PtMe_3(L\text{–}L)(pydz)][BF_4]$ (L–L = bipy, phen or bipym).

Table 4 Eyring and Arrhenius activation parameters* for the complexes $[PtMe_3(L\text{–}L)(pydz)][BF_4]$ (L–L = bipy, bipym, phen or tmen)

Complex (L–L)	E_a/kJ mol^{-1}	$\log_{10}(A/s^{-1})$	$\Delta H^{\ddagger}$/kJ mol^{-1}	$\Delta S^{\ddagger}$/J K^{-1} mol^{-1}	$\Delta G^{\ddagger}$/kJ mol^{-1}
bipy	85.3 (8.0)	14.8 (1.4)	82.8 (8.0)	29.1 (26.4)	74.2 (0.1)
bipym	117.3 (7.3)	19.7 (1.2)	114.7 (7.3)	123.9 (23.5)	77.7 (0.3)
phen	90.8 (6.2)	15.3 (1.1)	88.8 (6.2)	38.6 (20.0)	76.7 (0.3)
tmen	118.1 (4.5)	23.3 (0.9)	115.9 (4.5)	193.0 (17.0)	58.3 (0.6)

* Errors given in parentheses; $\Delta G^{\ddagger}$ quoted at 298.15 K.

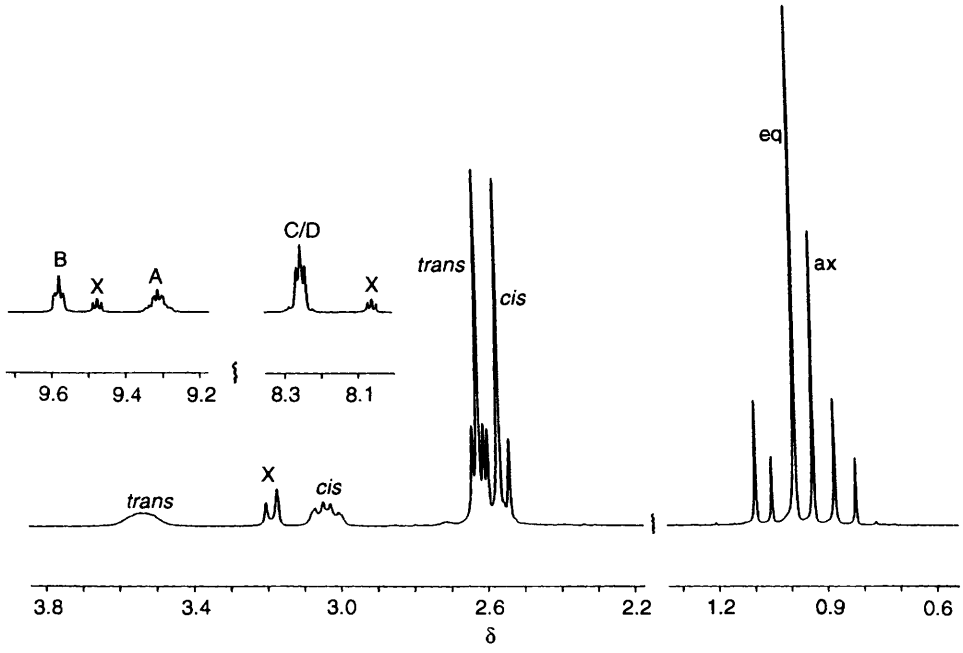

Fig. 3 The 250 MHz ^{1}H NMR spectrum of $[PtMe_3(tmen)(pydz)][BF_4]$ in $(CD_3)_2CO$ solution at 253 K. Minor product species denoted by X

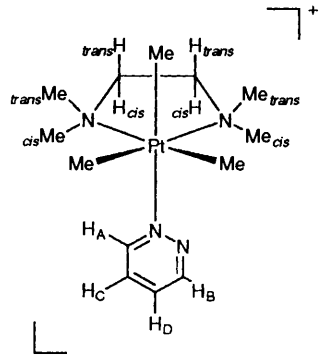

Scheme 3 The complex $[PtMe_3(tmen)(pydz)][BF_4]$ showing the hydrogen labelling

Discussion

The activation parameters determined for the 1,2-Pt–N fluxional shift in the complexes $[PtMe_3(L\text{–}L)(pydz)][BF_4]$ (L–L = bipy, phen, bipym or tmen) are reported in Table 4. Examination of the magnitudes of the free energies of activation, $\Delta G^{\ddagger}$ (298 K), reveals a dependence on the chelate ligand, the trend in $\Delta G^{\ddagger}$ being bipym > phen > bipy > tmen. This relationship may be rationalised in terms of a decrease in the Pt–N (pydz) interaction concomitant with an increase in the Pt–N (chelate ligand) interaction, and would therefore be expected to be in accord with the trend in the relative *trans* influences of the chelate ligands. An indication of the relative *trans* influences of the ligands (L–L = bipy, phen, bipym or tmen) can be obtained[22,23] by comparison of the ^2J(PtH) scalar couplings associated with the equatorial platinum methyls, the observed trend in $^2J(Pt\text{–}CH_{eq})$ values being bipym > phen > bipy > tmen (Table 2). This implies that the *trans* influence increases from tmen to bipym. Thus, as the *trans* influence of the chelate ligand increases, so the Pt–N (pydz) interaction decreases, leading to a slight destabilisation of the ground state and a lowering of the free energy of activation. The observed trend in $\Delta G^{\ddagger}$ (298 K) is also in accord with the pK_a values of the free L–L, *i.e.* $\Delta G^{\ddagger}$ increases as the pK_a decreases. However, it should be noted that the pK_a values are not generally a reliable indication of the relative co-ordinating abilities of ligands.[1]

Since the chelate ligands have a *cis* relationship with the fluxional Pt–N (pydz) bond no strong dependence was anticipated, and the substantially lower magnitude of $\Delta G^{\ddagger}$ (298 K) observed for the *N*,*N*,*N*′,*N*′-tetramethylethylenediamine complex $[PtMe_3(tmen)(pydz)][BF_4]$, cannot be rationalised solely in terms of a strong Pt–N (tmen) interaction. It seems probable that there is also a strong steric interaction between the two *cis* *N*-methyl groups of tmen and the pyridazine ring, giving rise to further weakening of the Pt–N (pydz) bond interaction and a substantial lowering of the free energy of activation.

The $\Delta G^{\ddagger}$ (298 K) values obtained for the 1,2-Pt–pydz metallotropic shift in the present complexes $[PtMe_3(L\text{–}L)(pydz)][BF_4]$ (L–L = bipy, phen or bipym), are *ca.* 4–8 kJ mol^{-1} greater than those obtained for the bis (pyridazine) complexes $[PtXMe_3(pydz)_2]$ (X = Cl, Br or I).[6] This increase may result either from a slight lowering of the ground-state energy or a slight increase in the transition-state energy. It is not possible to differentiate between these two possibilities by NMR methods. However, the platinum–pyridazine bond strength would be expected to increase on co-ordination to a

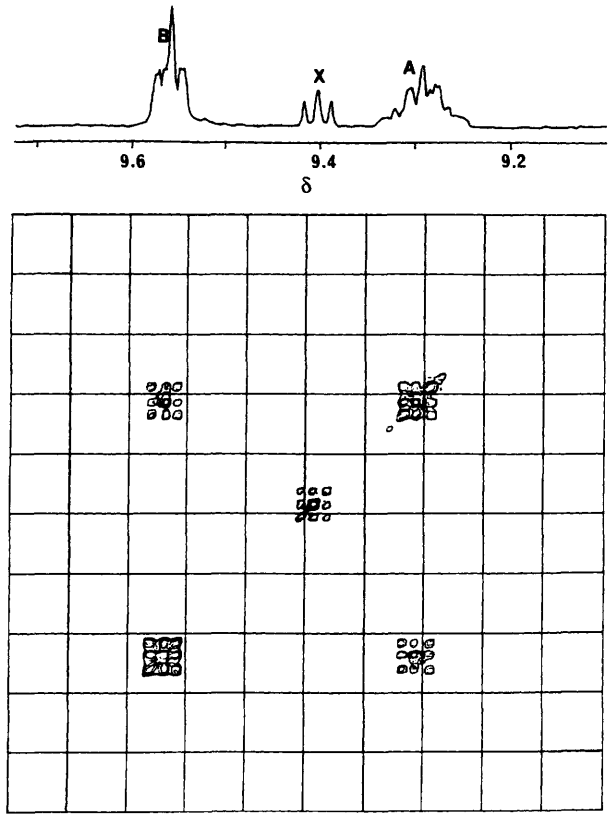

Fig. 4 The 250 MHz ^1H two-dimensional EXSY spectrum of $[PtMe_3(tmen)(pydz)][BF_4]$ at 258 K, showing exchange between the pydz hydrogens H_A and H_B. Minor product species denoted by X

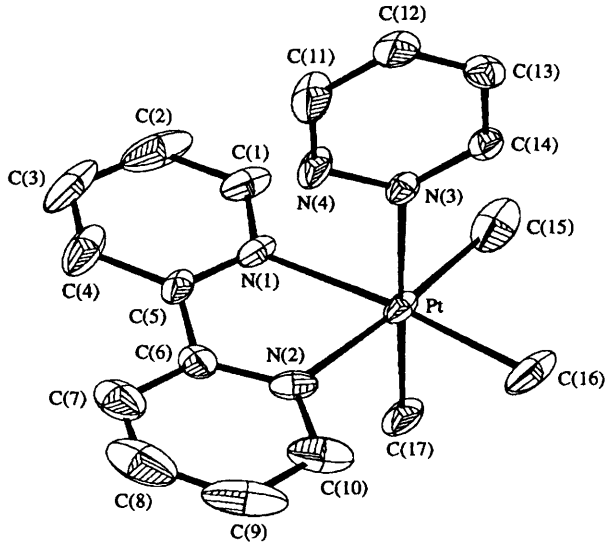

Fig. 5 Molecular structure of the $[PtMe_3(bipy)(pydz)]^+$ cation showing the atom labelling scheme. Hydrogen atoms have been omitted for clarity

complex cation, such as $[PtMe_3]^+$, which tends to suggest that the greater $\Delta G^‡$ values observed for the present complexes result from a slight stabilisation of the ground-state energy of the Pt–N (pydz) bond.

The mechanism of the 1,2-metal–pyridazine shift has been discussed extensively.[5,6,8,24,25] Two extreme transition states can be envisaged, *viz.* (*i*) a N,N′-σ-bonded 20-electron transition state, characterised by long Pt–N interactions and (*ii*) a π-bonded 18-electron transition state in which the metal–

Table 5 Selected bond lengths (Å) and angles (°) for $[PtMe_3(bipy)(pydz)][BF_4]$

Pt–C(15)	2.07(2)	Pt–C(16)	2.09(1)
Pt–C(17)	2.07(1)	Pt–N(1)	2.16(1)
Pt–N(2)	2.13(1)	Pt–N(3)	2.21(1)
C(17)–Pt–C(15)	87.7(5)	C(17)–Pt–C(16)	86.8(5)
C(15)–Pt–C(16)	86.4(6)	C(17)–Pt–N(2)	92.6(4)
C(15)–Pt–N(2)	175.6(5)	C(16)–Pt–N(2)	98.0(5)
C(17)–Pt–N(1)	92.8(4)	C(15)–Pt–N(1)	100.3(5)
C(16)–Pt–N(1)	173.3(5)	N(2)–Pt–N(1)	75.3(4)
C(17)–Pt–N(3)	178.6(4)	C(15)–Pt–N(3)	91.2(5)
C(16)–Pt–N(3)	92.3(4)	N(2)–Pt–N(3)	88.6(3)
N(1)–Pt–N(3)	88.2(3)	C(5)–N(1)–Pt	115.5(7)
C(1)–N(1)–Pt	123.4(9)	C(6)–N(2)–Pt	116.7(7)
C(10)–N(2)–Pt	122.5(11)	N(4)–N(3)–Pt	115.1(6)
C(14)–N(3)–Pt	123.5(7)		

Table 6 Atomic coordinates ($\times 10^4$) for $[PtMe_3(bipy)(pydz)][BF_4]$

Atom	*x*	*y*	*z*
Pt	1 553(1)	102(1)	8 144(1)
N(1)	1 262(4)	−1 430(7)	8 780(6)
C(1)	787(5)	−2 144(11)	8 413(9)
C(2)	614(8)	−3 046(14)	8 827(15)
C(3)	938(10)	−3 252(15)	9 684(14)
C(4)	1 390(8)	−2 522(13)	10 028(10)
C(5)	1 568(5)	−1 618(10)	9 567(7)
N(2)	2 174(4)	18(8)	9 356(7)
C(6)	2 078(5)	−822(12)	9 892(7)
C(7)	2 414(7)	−971(16)	10 697(10)
C(8)	2 852(10)	−221(22)	10 964(14)
C(9)	3 019(8)	694(18)	10 415(17)
C(10)	2 647(5)	777(12)	9 579(11)
N(3)	1 023(3)	1 379(7)	8 683(5)
N(4)	1 005(5)	1 095(8)	9 449(6)
C(11)	688(7)	1 829(13)	9 796(8)
C(12)	409(5)	2 893(11)	9 411(8)
C(13)	431(5)	3 149(10)	8 628(8)
C(14)	752(4)	2 383(9)	8 283(7)
C(15)	916(8)	71(9)	6 993(10)
C(16)	1 921(6)	1 595(11)	7 652(10)
C(17)	2 045(5)	−1 071(10)	7 611(7)
B	−962(5)	5 266(12)	8 324(7)
F(1)	−501(5)	5 215(9)	9 003(7)
F(2)*	−1 148(12)	4 083(16)	8 335(13)
F(3)*	−759(27)	5 399(51)	7 657(26)
F(4)*	−1 367(24)	6 122(49)	8 016(35)
F(2′)*	−1 443(11)	5 299(39)	8 564(26)
F(3′)*	−798(14)	4 949(34)	7 646(13)
F(4′)*	−903(20)	6 514(16)	8 407(26)

* Atom refined with fixed partial occupancy of 0.5.

nitrogen distances are approximately equal to the ground-state M–N distance.[24] The sizeable $\Delta S^‡$ values observed for the complexes $[W(CO)_5(pydz)]$[5] and $[PtXMe_3(pydz)_2]$[6] suggested a transition state characterised by long M–N distances, *i.e.* one which more closely approximates to a 20- than an 18-electron intermediate. The magnitudes of the $\Delta S^‡$ values obtained for the present complexes also tend to suggest a 20-electron type intermediate, with long Pt–N distances. The anomalously high $\Delta S^‡$ value observed for $[PtMe_3(tmen)(pydz)][BF_4]$ lends support to the presence of a large steric interaction between the *N*-methyls of the chelate ligand and the pyridazine ring, and contributes significantly to the lowering of the energy barrier of the 1,2-Pt–N shift as measured by the $\Delta G^‡$ parameter (see above).

Crystal Structure of $[PtMe_3(bipy)(pydz)][BF_4]$.—The crystal structure consists of discrete $[PtMe_3(bipy)(pydz)]^+$ cations and $[BF_4]^-$ anions held together by van der Waals interactions.

The structure of the cation, shown in Fig. 5, clearly reveals the expected *fac*-octahedral co-ordination of the $PtMe_3$ moiety and monodentate co-ordination of the pyridazine ligand. The Pt–N (pydz) and Pt–Me bond lengths [2.21(1) and 2.07–2.09(1) Å respectively] are marginally longer than the corresponding values [2.178, 2.190(4) and 2.038–2.077(7) Å] in the related complex $[PtClMe_3(pydz)_2]$,[6] but the differences are statistically insignificant. The pydz ligand is oriented in such a way that the ring plane approximately bisects the N(1)–Pt–N(2) and C(15)–Pt–C(16) angles and the unco-ordinated nitrogen lies on the side of bipyridyl. Deviations from idealised octahedral geometry are substantial, mainly due to the small bite size of bipyridyl [N(1)–Pt–N(2) 75.3(4)°], which opens up the N(1)–Pt–C(15) and N(2)–Pt–C(16) *cis* angles to 100.3(5) and 98.0(5)° respectively, and narrows down the N(1)–Pt–C(16) and N(2)–Pt–C(15) *trans* angles to 173.3(5) and 175.6(5)° respectively. Other angular distortions are mostly consistent with the requirement of minimum interligand non-bonded interactions. The dimensions of the ring systems are as expected.

Acknowledgements

We are grateful to the University of Exeter for a studentship (to P. J. H.) and to the EPSRC for the mass spectrometry and X-ray crystallography services.

References

1 G. Wilkinson, R. D. Gillard and J. A. McCleverty (Editors), *Comprehensive Coordination Chemistry*, Pergamon, New York, 1987, vol 2, p. 73 *et seq.*
2 S. S. Eaton, G. R. Eaton and R. H. Holm, *J. Organomet. Chem.*, 1972, **39**, 179.
3 K. R. Dixon, *Inorg. Chem.*, 1977, **16**, 2618.
4 M.-J. Bermejo, J.-I. Ruiz and J. Vinaixa, *Transition Met. Chem.*, 1987, **12**, 179.
5 E. W. Abel, E. S. Blackwall, K. G. Orrell and V. Šik, *J. Organomet. Chem.*, 1994, **464**, 163.
6 E. W. Abel, E. S. Blackwall, P. J. Heard, K. G. Orrell, V. Šik, M. B. Hursthouse, M. A. Mazid and K. M. A. Malik, *J. Chem. Soc., Dalton Trans.*, 1994, 445.
7 E. W. Abel, P. J. Heard, K. G. Orrell and V. Šik, *Polyhedron*, 1994, **13**, 2907.
8 P. J. Heard, Ph. D. Thesis, University of Exeter, 1994.
9 J. C. Baldwin and W. C. Kaska, *Inorg. Chem.*, 1975, **14**, 2020.
10 D. H. Goldsworthy, Ph. D., Thesis, University of Exeter, 1980.
11 D. E. Clegg, J. R. Hall and G. A. Swile, *J. Organomet. Chem.*, 1972, **38**, 403.
12 D. F. Shriver, *Manipulation of Air-sensitive Chemicals*, McGraw-Hill, New York, 1969.
13 D. D. Perrin and W. L. F. Armarego, *Purification of Laboratory Chemicals*, Pergamon, Oxford, 1985.
14 G. Bodenhausen, H. Kogler and R. R. Ernst, *J. Magn. Reson.*, 1984, **58**, 370.
15 E. W. Abel, T. P. J. Coston, K. G. Orrell, V. Šik and D. Stephenson, *J. Magn. Reson.*, 1986, **70**, 34.
16 G. Binsch and H. Kessler, *Angew. Chem., Int. Ed. Engl.*, 1980, **19**, 411.
17 J. A. Darr, S. R. Drake, M. B. Hursthouse and K. M. A. Malik, *Inorg. Chem.*, 1993, **32**, 5704.
18 SHELXS, G. M. Sheldrick, *Acta Crystallogr., Sect. A*, 1990, **46**, 467; SHELXL 93, G. M. Sheldrick, University of Göttingen, 1993; DIFABS, N. P. C. Walker and D. Stuart, *Acta Crystallogr., Sect. A*, 1983, **39**, 158; SNOOPI, K. Davies, University of Oxford, 1983.
19 A. J. Downs, D. A. Long and L. A. K. Staveley (Editors), *Essays in Structural Chemistry*, Macmillan, London, 1971, p. 433.
20 A. Psaila, Ph. D. Thesis, University of Exeter, 1977.
21 E. W. Abel, S. K. Bhargava and K. G. Orrell, *Prog. Inorg. Chem.*, 1984, **32**, 1.
22 G. W. Smith, *J. Chem. Phys.*, 1963, **39**, 2031.
23 G. W. Smith, *J. Chem. Phys.*, 1965, **42**, 435.
24 S.-K. Kang, T. A. Albright and C. Mealli, *Inorg. Chem.*, 1987, **26**, 3158.
25 S. Alvarez, M.-J. Bermejo and J. Vinaixa, *J. Am. Chem. Soc.*, 1987, **109**, 5136.

Received 2nd May 1995; *Paper* 5/02805A